EIDGENÖSSISCHE TECHNISCHE HOCHSCHULE LAUSANNE
POLITECNICO FEDERALE LOSANNA
SWISS FEDERAL INSTITUTE OF TECHNOLOGY

SECTION MICROTECHNIQUE

ÉCOLE POLYTECHNIQUE
FÉDÉRALE DE LAUSANNE

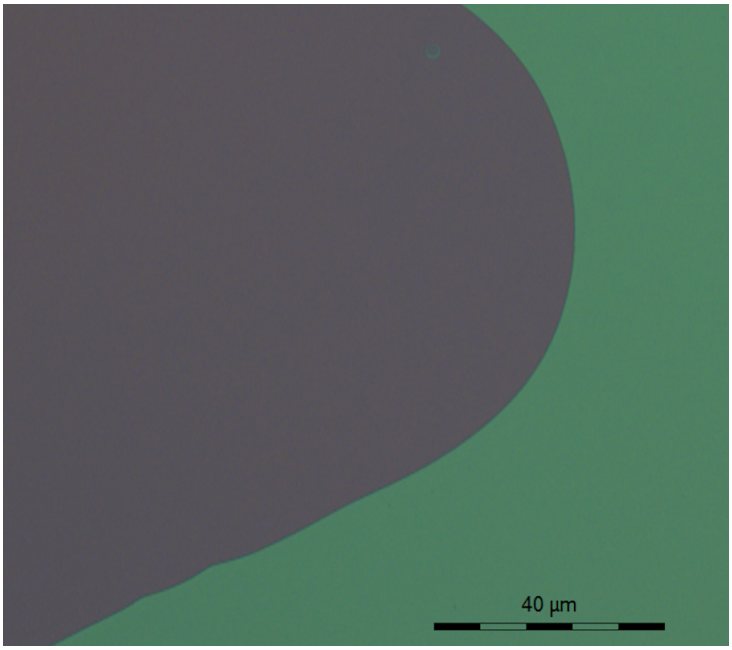

Optimization of sputter deposition Process for piezoelectric AlN ultra-thin Films

Semester Project
Advanced NEMS group
Autumn Semester 2017

Roman Welz
January 23, 2018

Supervisor:
Kaitlin Howell

Professor:
Prof. Luis Guillermo Villanueva

Optimization of sputter deposition Process for piezoelectric AlN ultra-thin Films

Welz, Roman, Section Microtechnique

Assistant: *Kaitlin Howell*

Professor: *Luis Guillermo Villanueva*

The sputtering conditions for the deposition of the layers underneath active AlN films were analyzed for improving the quality of the active AlN, and the dependence of AlN deposition temperature on crystalline quality was investigated, where a reduced deposition temperature could reduce the process time and cost. Therefore wafers with a 25 nm bottom electrode on a 15 nm adhesion layer, a 100 nm piezoelectric AlN film and a 100 nm top electrode have been deposited using different metals (Mo, Pt and Al) as bottom electrodes, different seed layers (Ti and AlN) and were deposited in two different sputtering machines. For the Mo bottom electrode, the sputtering power has also been varied between 250W, 500W, 750W and 1000W, and the deposition rates for these powers have been determined. The thickness, resistivity, rocking curve FWHM and stress have been measured for the bottom electrodes. The stress has been analyzed for the seed layers and for the AlN and top electrode layers and the rocking curve FWHM for the AlN has been measured and studied. Three structures with a Pt bottom electrode on a Ti seed layer have been created, where the active AlN film has been deposited at 300°C, 150°C and at room temperature respectively. It was shown, that AlN layers deposited on Pt bottom electrodes showed the best crystalline quality of the metals tested and the active AlN quality showed no significant difference, whether it was deposited at 150°C or 300°C.

Contents

1 Introduction

A large number of applications rely on piezoelectric thin films. They are for example often used in telecommunications for RF band pass filters and for sensing. Out of the many piezoelectric materials, aluminum nitride (AlN) has become one of the most used in the field of MEMS. It is of particular interest, since it can be integrated with standard CMOS applications. It is chemically compatible with semiconductor materials and can be deposited at rather low temperatures required by CMOS processes, which often need to stay below 500°C [2]. Although AlN can be deposited by many different deposition methods, reactive magnetron sputtering is commonly used in MEMS applications, since it allows deposition of AlN films at moderate temperatures [10].

In a magnetron sputtering configuration a target (Al for AlN deposition) is mounted on a cathode and the substrate is fixed on the anode. A vacuum (in the order of 10^{-3} mbar) is established in the vacuum chamber and an argon gas is introduced. Two configurations exist, DC and RF sputtering. In this project only DC sputtering was used, where a DC voltage is applied between the target and substrate. This voltage produces a plasma in which ionized Ar atoms get accelerated and impinge on the target. The impinging ions eject particles from the target towards the substrate, where they form a growing film. Figure 1(a) shows a schematic of such a system. In this figure the substrate is fixed on the anode on top and the target on the cathode on the bottom. The distance between substrate and target is usually only a couple of centimeters, which leads to a rather uniformly deposited film. AlN is deposited in reactive DC pulsed sputtering, where the reaction gases are Ar and N_2. Nitrogen reacts with the aluminum to form AlN. The quality of the sputtered film depends on the different conditions used during the process, such as the power, substrate temperature, pressure in the chamber and Ar/N_2 gas ratio. [10] Varying these conditions, changes the stress in the deposited film [2]. In magnetron sputtering, magnets are used to improve the deposition.

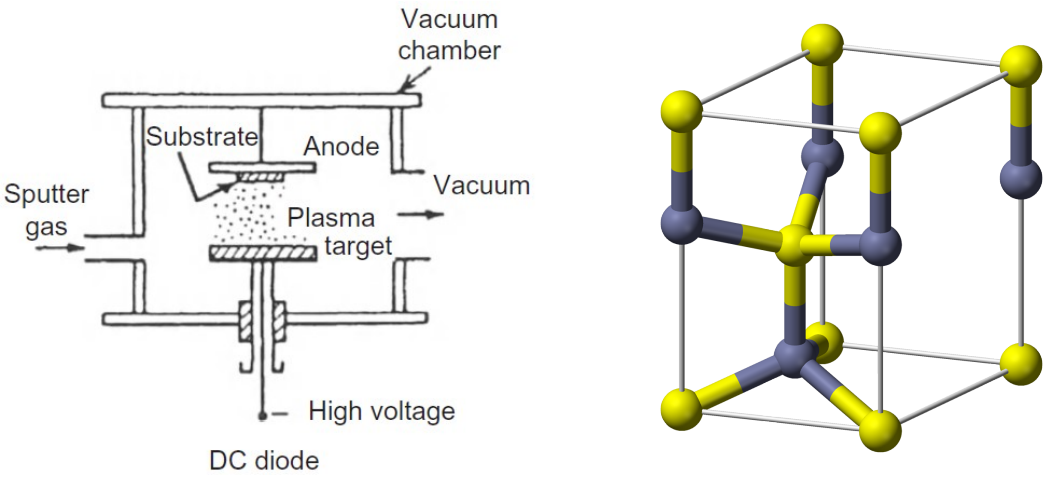

Figure 1: *Schematics showing (a) the sputtering process (from [13]) and (b) the wurtzite crystal structure*

AlN grows in a wurtzite structure, which is shown in Figure 1(b). The c-axis (vertical axis in the image) is polar. AlN films can have two polarities, either Al- or N-polar, which determine the sign of the piezoelectric coefficient. In films grown by DC pulsed magnetron sputtering, N-polarity

is more pronounced. For a good quality piezoelectric AlN film, a strong polarity is required. It was found, that AlN films grown by sputtering are composed of densely packed columnar grains that exhibit a strong c-axis (0001) orientation [10] [2]. The best quality piezoelectric AlN films were grown on substrates exhibiting a hexagonal symmetry, such as (111) Pt or (111) Al. The large lattice mismatch between AlN and Pt was found not to influence the AlN quality. [2] [8] Martin et al. investigated the growth of AlN films on (110) molybdenum substrates, which shows no hexagonal symmetry and deposited AlN films on optimized Mo. They found a requirement for a high deposition power, elevated substrate temperature and low Ar gas flow rate for an optimal Mo deposition [8]. Dubois et al. studied the influence of substrate materials, comparing piezoelectric AlN quality on (111) Pt, (111) Al and (0002) Ti. AlN films grown on the latter two only showed a moderate piezoelectric quality, whereas films grown on Pt gave the best results [2]. They also found a large influence of the deposition conditions, where atoms and molecules arriving onto the growing AlN film need to have a certain energy. This is in agreement with what was found by Jin et al. [5]. They tested the influence of the substrate temperature during the deposition and found an optimal value of 430°C. Ivanov et al. only found that a higher substrate temperature produced a better quality AlN film [3]. Other parameters that have an influence on the AlN film are the deposition power, as well as the bias applied to the substrate during deposition. It is also interesting to note that the thickness of the AlN film has an infuence on the crystalline and piezoelectric quality [9]. A correlation between these last two was found by Martin et al. and Loebl et al., showing that a reduced AlN rocking curve full width at half maximum (FWHM) resulted in an increased piezoelectric coefficient $d_{33,f}$ [9] [7].

In this work the influence of different substrates was tested by depositing AlN on (110) Mo, (111) Pt and (111) Al electrodes, where the deposition power of the Mo films has been varied. For optimizing the electrode film underneath the AlN film, it is interesting to study the influence of the adhesion layer as well as the underlying substrate. Although many works showed a better AlN quality for deposition at high temperature, an attempt at reducing this temperature was also made.

2 Methods

In the scope of this project, 3 sets of depositions have been performed, the first for determining the sputtering rate of molybdenum films, the second for determining the active AlN quality for AlN films deposited onto different bottom electrode films and the third for determining the active AlN quality deposited on different underlying layers, different adhesion layers between the metal and the substrate, metal layers deposited by two different sputtering machines and for different deposition temperatures for the active AlN layers.

Throughout the whole project (100) Si wafers have been used with a diameter of 100 mm and a thickness of 525 μm. Some of these wafers had an additional 200 or 300 nm thick wet SiO_2 layer on top (SiO_2 wafers). In one case a wafer was used with a Si_3N_4 interfacial layer on top of the Si (Si_3N_4 wafer).

2.1 Sputter deposition

Two different sputter deposition machines were used. Most depositions were performed using the Pfeiffer Vacuum Spider 600. This machine has four independent sputter deposition chambers.

One of which can be used for RF sputtering. However for this work all depositions were made by DC magnetron sputtering. Additionally to Ar, N_2 gas was introduced to the chamber for deposting the AlN films. The purity of the targets used was 99.99% for Mo, 99.95% for Pt, 99.9995% for Al, 99.995% for Ti and 99.9995% for the Al used in the AlN deposition, which was not the same as used in the Al deposition. Before performing a set of depositions, all targets were cleaned by sputtering onto a designated cleaning wafer. The Alliance-Concept DP650 sputtering machine was used to deposit 4 wafers. This machine was operated by Kaitlin Howell. Unlike the Spider, this machine has a mechanical shutter to cover the substrate. It only has one deposition chamber, which contains 6 targets inside. It was only used to deposit Ti adhesion films and Al, Mo and Pt bottom electrode films by DC magnetron sputtering.

2.2 Stress measurement

The stress has been determined by measuring the curvature of the wafer before and after deposition of the films. For all wafers the curvature was measured before depositing any layers. The ones with only one layer had the curvature measured after this deposition and the wafers with four layers had the curvature measured after deposition of the bottom electrode and again after deposition of the top electrode. The stress can then be calculated using Stoney's formula [1]

$$\sigma = \frac{E_{subst}}{6(1-\nu_s)}\frac{t_s^2}{t_f}\cdot\left[\frac{1}{R}-\frac{1}{R_0}\right] \tag{1}$$

where E_{subst} is the substrates Young's modulus, ν_s the substrates Poisson's ratio, t_s is the substrate thickness, t_f the film thickness and R_0 and R the radius of curvature measured before and after the deposition respectively. The ratio $\frac{E_{subst}}{(1-\nu_s)} = 180.5\ GPa$ and the substrate thickness is $t_s = 525\mu m$. In order to obtain the stress in the bottom electrode layer, it is necessary to perform stress deconvolution using the formula

$$\sigma_{be} = \frac{\sigma_{sl+be}t_{sl+be} - \sigma_{sl}t_{sl}}{t_{be}} \tag{2}$$

where σ_{sl} and t_{sl} denote the stress and thickness of the seed layer respectively, σ_{be} and t_{be} the bottom electrode stress and thickness respectively and σ_{sl+be} and t_{sl+be} the stress and thickness of both those layers [12]. Similarly we can calculate the stress in the active AlN and top electrode metal layer

$$\sigma_{AlN+te} = \frac{\sigma_{4layers}t_{4layers} - \sigma_{sl}t_{sl} - \sigma_{be}t_{be}}{t_{AlN+te}} \tag{3}$$

where $AlN{+}te$ stands for the active AlN and top electrode layers combined and $4layers$ for all 4 layers combined, *be* for bottom electrode and *sl* for the seed layer. The wafers with only a seed layer were deposited with the goal of measuring the thickness and residual stress of this layer. The calculation of the standard deviation can be found in Appendix D.

2.3 Thickness measurement

Before depositing the seed layer, the wafers were prepared by tracing three lines on each of them with an ink pen. After depositing the bottom electrode, a lift-off is performed on this area. To this end, on the wet bench in zone 13 of the cleanroom, the wafers were immersed in a beaker filled with isopropyl alcohol (IPA), which etches away the ink. The side with the deposited

layers face down, so that the released particles fall to the ground rather than stick to the wafer. The beaker is placed in an ultrasonic bath in order to accelerate the etching process. After a few minutes the beaker is taken out of the ultrasonic bath and the remaining material is removed by light scrubbing with a cleanroom swab, while keeping the wafer inside the IPA with the metal side facing down. The wafer is once again put in the ultrasonic bath, before being rinsed with deionized (DI) water and dried with a nitrogen gun.

The lift-off produced a step on the wafer surface with a depth corresponding to the thickness of the deposited films. The Bruker DektakXT is a surface profilometer used to measure the height of steps on the surface. It uses a stylus with a size of $12.5\mu m$. In this project the DektakXT was set to move over a distance of $75\mu m$, for a duration of 60 seconds with a resolution of $0.004\mu m$. The range was set to $6.5\mu m$. For the wafers 68732 and 68737 (Ti seed layer only) the measurement was performed over a length of $150\mu m$ for a time of 120 seconds. The resolution and range were kept the same as before. For each wafer a set of four measurements has been performed.

Due to its superior precision, the thickness of the AlN seed layer was measured on the Sopra GES 5E spectroscopic ellipsometer. The ellipsometer allows for an accurate measurement of transparent thin film thickness. It measures the change of polarization of light reflected at non-normal incidence on the transparent film. [11]

2.4 Resistivity measurement

Another parameter of interest was the resistivity of the bottom electrode metal. In order to determine this, the KLA-Tencor OmniMap RS75 was used to measure the sheet resistance. The OmniMap is a four point resistivity measurement tool. It was used to measure the sheet resistance at 49 points distributed over the wafer. The resistivity ρ can be obtained by multiplying the sheet resistance R_s of the film with its thickness t_f.

$$\rho = R_s \cdot t_f \tag{4}$$

The calculation of the corresponding standard deviation can be found in Appendix D.

2.5 Oxide thickness measurement

Using the Nanospec AFT-6100 spectroscopic reflectometer, the thickness of the SiO_2 layer was measured over 49 points on the wafer. On most SiO_2 wafers the oxide thickness was checked in order to verify the quality and uniformity of this interfacial layer.

2.6 X-ray diffraction

X-ray diffractometry (XRD) was used to determine the crystal structure of the sample in question. Using Bragg's law the distance between two crystal layers can be determined from the angle of peak reflection. In this work two methods of x-ray diffractometry have been used, $\theta/2\theta$ and rocking curve. In $\theta/2\theta$ mode the reflection was measured at the same angle as the x-rays were sent in. In rocking curve mode the angle between the x-ray gun and the detector is kept constant at the peak reflection angle for the crystal orientation of interest and the two are rotated around this peak. A direct relation between the rocking curve FWHM and the piezoelectric quality of

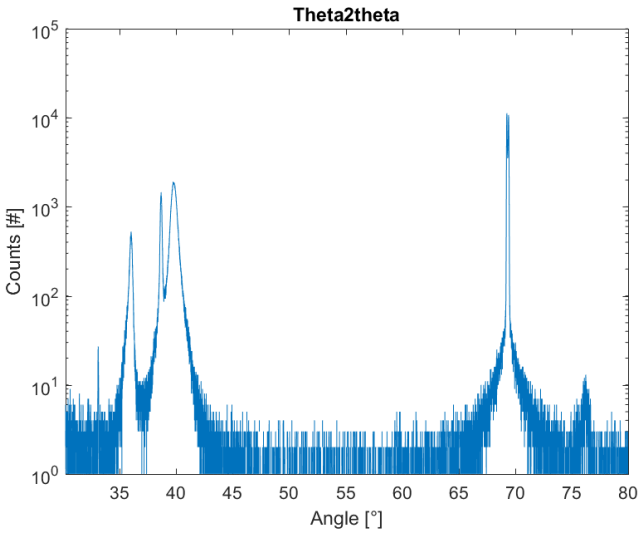

Figure 2: *The $\theta/2\theta$ scan of the wafer 68733. At around 36 ° the AlN (0002) diffraction peak can be observed. The Pt (111) and Al (111) peaks are at around 40 ° and the largest peak around 69 ° originates from the Si (400) substrate.*

the AlN film was found by Loebl et al. [7] and Martin et al. [9]. An increase in the rocking curve FWHM leads to a decrease of the piezoelectric coefficient $d_{33,f}$ and the coupling constant k_t^2. Therefore the Bruker X-ray diffractometer was used to measure the AlN rocking curve and since the interest of this work is to see the influence of the bottom electrode on the piezoelectric quality of the AlN film, the rocking curve of the bottom electrode metal was also measured.
For measuring the rocking curve FWHM a $\theta/2\theta$ scan was performed from 30° to 80°. Figure 2 shows such a $\theta/2\theta$ scan obtained for the wafer 68733. In this scan the AlN (0002) peak has to be identified ($\sim$ 36°) and a rocking curve measurement performed around it. A rocking curve measurement has been performed around the bottom electrode peak as well ($\sim$ 39.8° for Pt (111) and $\sim$ 40.4° for Mo (110)). To estimate the rocking curve FWHM a Gaussian distribution was fitted to the rocking curve measurement and its FWHM determined.

2.7 Molybdenum sputter deposition speed

In the first set of depositions molybdenum was sputtered onto (100) Si wafers. Four depositions have been realized with a sputtering power of 250W, 500W, 750W and 1000W respectively. The deposition time was set to 60 seconds in each case. The Pfeiffer Vacuum Spider 600 further explained in Section 2.1 was used for all depositions. A lift-off was performed producing a step throughout the deposited layers. Using the Bruker DektakXT profilometer, this step could be measured and therefore the thickness and the deposition rate of the film determined. The whole process of the thickness measurement is explained in detail in Section 2.3. The film stress has been determined by using the Toho Technology FLX 2320-S explained in Section 2.2.

2.8 Active AlN on different bottom electrodes

A set of depositions was performed, where structures were deposited as shown in Figure 3. Table 1 summarizes the deposition conditions of these wafers. All wafers had an AlN adhesion layer.

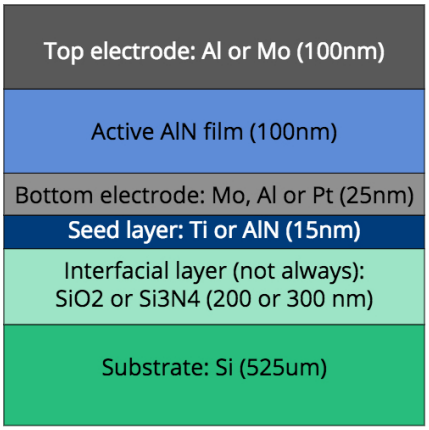

Figure 3: *A schematic of the deposited cross section*

The last three wafers in the table (66210, 73954 and 63228) had nothing but the seed layer deposited. Three different substrates were used. All wafers had a 25 nm bottom electrode, a 100 nm active AlN and a 100 nm top electrode with the exception of wafer 63229 (Pt on Si_3N_4), which had a 50 nm top and bottom electrode thickness and a 300 nm active AlN layer. The Si_3N_4 wafers had a polysilicon layer underneath the Si_3N_4, which made the surface a bit rougher. The top electrode metal has never been the same as the bottom electrode metal, so the peaks do not overlap in the XRD scan. As shown in Table 1 wafer 73955 had the same deposition conditions as wafer 66208, but a (100) Si substrate. Wafer 66209 had an Al bottom electrode and a Mo top electrode metal. The active AlN film was deposited the same for all wafers at 300°C with a deposition power of 1500 W, an Ar gas flow rate of 10 sccm and a N_2 gas flow rate of 40 sccm. Previous to the AlN deposition a RF etch was performed for 60 seconds. Stress, thickness and resistivity have been measured as described in Section 2.2, Section 2.3 and Section 2.4 respectively. The thickness has not been measured for the Pt on Si_3N_4 wafer and for any of the active AlN and top electrode layers. The thickness of these layers is known to have a standard deviation of $\pm 5\,nm$ from previous measurements by the ANEMS group. The rocking curve measurements of the AlN and the bottom electrode metal were performed in the XRD as described in Section 2.6.

By having wafers with nothing but a seed layer deposited, it was possible to measure the thickness and stress of these adhesion layers. Wafers with the seed layer deposited under the same conditions were assumed to be within the standard deviation. These measurements made it possible to find the stress and thickness of the bottom electrode film.

Wafer	Substrate	Bottom electrode metal	Top electrode metal	Deposition power bottom electrode	Deposition time bottom electrode
66208	SiO_2	Mo	Al	250 W	29 s
66207	SiO_2	Mo	Al	500 W	14 s
66216	SiO_2	Mo	Al	750 W	9 s
66218	SiO_2	Mo	Al	1000 W	7 s
66209	SiO_2	Al	Mo	200 W	44 s
63229	Si_3N_4	Pt	Mo	500 W	20 s
73955	Si	Mo	Al	250 W	29 s
66210	SiO_2	-	-	-	-
73954	Si	-	-	-	-
63228	Si_3N_4	-	-	-	-

Table 1: *Deposition conditions for the deposition of the bottom electrode metal in the second deposition*

2.9 Variation of seed layers and sputtering machines

In a third deposition the bottom electrode metal, the seed layer material and the sputter deposition machine were varied and compared. Table 2 gives an overview of the deposition parameters. The films were deposited as shown in Figure 3 with a $200\,nm$ thick SiO_2 interfacial layer. The seed and bottom electrode layers were deposited with the machine indicated in Table 2. For each seed layer and machine combination a set of four wafers were deposited, one with the seed layer only and one with an Al, Mo and Pt bottom electrode each. The Spider did not allow to deposit Ti and Al at the same time, since the two materials use the same chamber. Therefore no Al on Ti wafer was deposited in the Spider. The active AlN and the top electrode films have always been deposited in the Spider600. The active AlN layer was deposited the same as in the second deposition described in Section 2.8 (300°C, $1500\,W$, 10 sccm Ar gas flow rate and 40 sccm N_2 gas flow rate with a one minute RF etch previous to the deposition). Since the rocking curve measurements of the wafers from the second deposition were very bad (see Section 3.2), the target used for the deposition of the AlN film was thoroughly cleaned for three hours by the CMi cleanroom staff previous to the active AlN deposition. On all wafers the thickness and stress were measured as described in Section 2.3 and Section 2.2 respectively. The resistivity of the bottom electrode was measured in the OmniMap as described in Section 2.4 and the rocking curves for AlN and the bottom electrode were measured in the XRD as described in Section 2.6.

Wafer	Machine	Seed layer	Bottom electrode metal	Top electrode metal	Deposition power	Ar gas flow rate
74089	Spider	AlN	Al	Mo	200 W	15 sccm
74086	Spider	AlN	Mo	Al	250 W	5 sccm
74088	Spider	AlN	Pt	Al	500 W	5 sccm
68734	Spider	Ti	Mo	Al	250 W	5 sccm
68739	Spider	Ti	Pt	Al	500 W	5 sccm
68736	DP650	Ti	Al	Mo	400 W	
68735	DP650	Ti	Mo	Al	400 W	
74087	DP650	Ti	Pt	Al	250 W	
52442	Spider	AlN	-	-	-	-
68732	Spider	Ti	-	-	-	-
68737	DP650	Ti	-	-	-	-

Table 2: *Deposition parameters for the wafers when comparing different seed layers and sputtering machines. The deposition power and the Ar gas flow rate are given for the bottom electrode metal deposition.*

2.10 Active AlN deposition temperature variation

Since heating the deposition chamber to 300°C takes a lot of time, which results in an increased cost, it would be interesting to see if and how the quality deteriorates when depositing the active AlN layer at a lower temperature. Therefore two additional wafers have been deposited in the Spider, with a Ti seed layer and a Pt bottom electrode layer. They were deposited the same way as the wafer 68733 described in Section 2.9 and in Table 2 (15 nm Ti seed layer, 25 nm Pt bottom electrode, 100 nm active AlN and 100 nm Al top electrode). The substrate was also a Si (100) wafer with a 200 nm wet SiO_2 layer on top. The thickness of the seed layer and bottom electrode was not measured, but is assumed to be within the standard deviation given by the measurements of wafer 68739. Film stress and resistivity were measured the same way as for previous wafers. Wafer 68738 had the active AlN deposited at 150°C and wafer 68733 at room temperature. For both wafers the deposition power was 1500 W and the Ar and N_2 gas flow rates were 10 and 40 sccm respectively. The one minute RF etch was only performed for wafers 68738 and 68739, since the recipe used for the active AlN deposition at room temperature did not include this step. The deposition conditions for these and wafer 68739 are summarized in Table 3. The AlN and Pt rocking curves were again measured in the XRD as described in Section 2.6.

Wafer	Bottom electrode material	Deposition temperature	Deposition power	Ar gas flow rate	N_2 gas flow rate
68739	Pt	300°C	1500 W	10 sccm	40 sccm
68738	Pt	150°C	1500 W	10 sccm	40 sccm
68733	Pt	RT	1500 W	10 sccm	40 sccm

Table 3: *Deposition conditions when comparing different active AlN layer deposition temperatures. The deposition temperature, power and gas flow rates are given for the active AlN layer.*

3 Results

3.1 Molybdenum sputter deposition speed

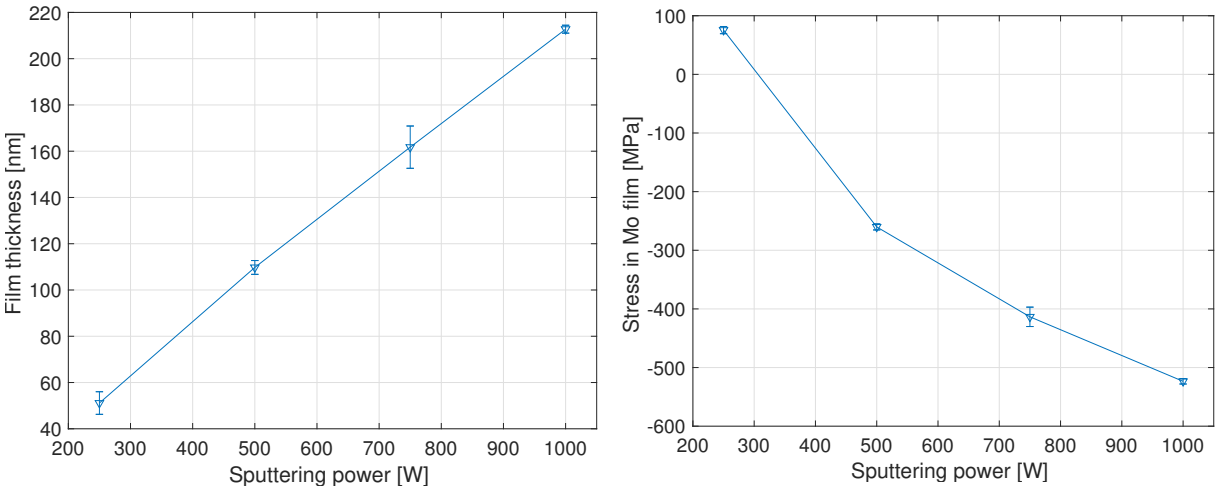

(a) *(b)*

Figure 4: *(a) The thickness of molybdenum layers deposited at different sputtering powers. The deposition time was kept constant at 60 seconds. (b) The resulting stress in the molybdenum layers deposited with different sputtering powers.*

The deposition of molybdenum layers with different sputtering powers resulted in the thicknesses presented in Figure 4(a). As expected, the thickness increases linearly with increasing deposition power. By dividing the measured thickness by the deposition time, the deposition rate for the different sputtering powers is obtained, which is summarized in Table 4. Figure 4(b) shows the stress in the molybdenum layers as a function of the deposition power. The stress in the layer deposited at 250W is tensile and compressive for larger deposition powers. It becomes more compressive for a higher sputtering power.

Sputtering power [W]	**Deposition speed [nm/minute]**
250	51 ± 5
500	110 ± 3
750	162 ± 9
1000	213 ± 2

Table 4: *The deposition speed of molybdenum for different sputtering powers*

3.2 Active AlN on different bottom electrodes

Figure 5 summarizes the results obtained from the second deposition, where active AlN layers were deposited on different bottom electrodes and with different substrates. Figure 5(c) shows the rocking curve FWHM obtained for the bottom electrodes and for AlN. All wafers produced bad rocking curve FWHM. The Pt on Si_3N_4 on polysilicon clearly showed the largest rocking curve FWHM, both for the bottom electrode and AlN. The Mo on SiO_2 wafer shows the smallest

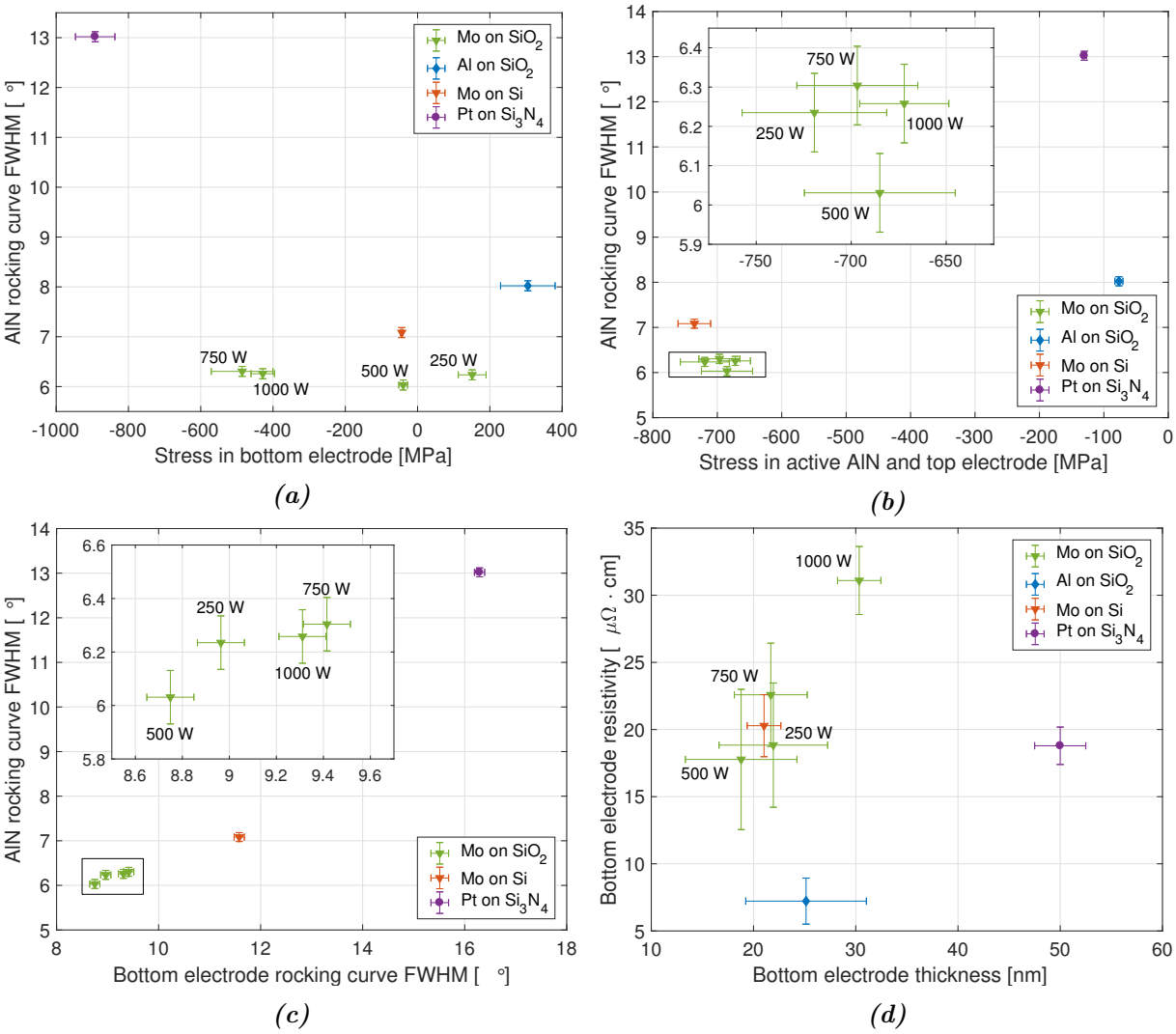

Figure 5: *The AlN rocking curve FWHM plotted against (a) stress in the bottom electrode and (b) stress in the active AlN and top electrode layer. (c) The AlN rocking curve FWHM as a function of the bottom electrode rocking curve FWHM. The black rectangles in (b) and (c) mark the area shown in the insets. (d) The resistivity in the bottom electrode layer compared to the thickness of the bottom electrode layer. The numbers in (a), (b), (c) and (d) indicate the desired sputtering power for the Mo bottom electrodes (green points).*

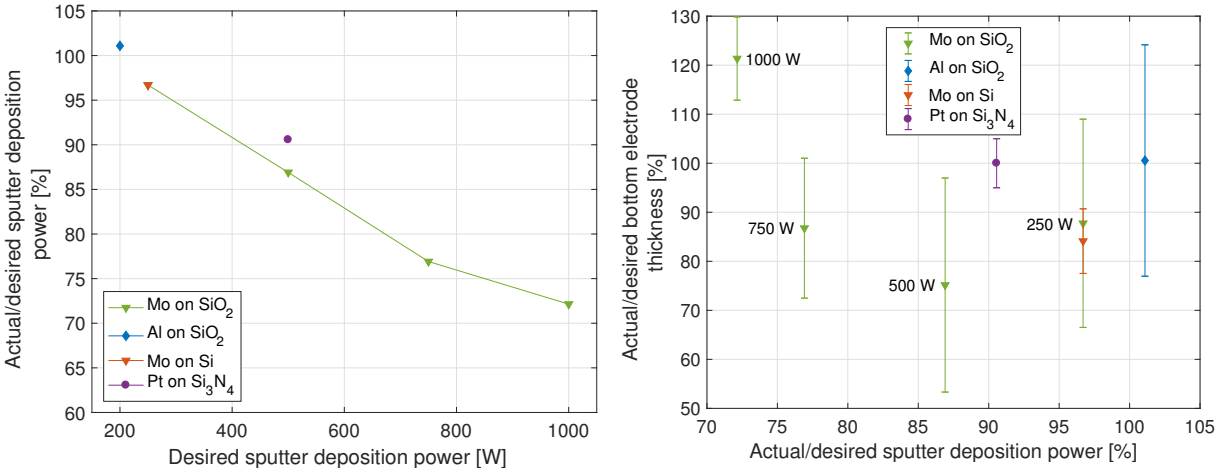

Figure 6: *(a) The actual mean sputter deposition power of the bottom electrode relative to its desired sputtering power as compared to the desired sputtering power. (b) The relative sputtering power compared to the actual bottom electrode thickness relative to the desired thickness. The numbers indicate the desired sputtering power for the Mo bottom electrodes (green points). The Pt bottom electrode thickness has not actually been measured.*

rocking curve FWHM. The rocking curve values change very little between the different deposition powers. The Al bottom electrode peak in the $\theta/2\theta$ scan was not pronounced enough, to permit a measurement of its rocking curve. The AlN rocking curve FWHM produced for the Al wafer, seen in Figure 5(a) is larger than for Mo bottom electrodes. This figure depicts the AlN rocking curve FWHM as a function of the stress in the bottom electrode film. In the Mo on SiO_2 films, the stress becomes more compressive with increasing deposition power. In the film deposited at 750 W, the standard deviation is high ($\sim 18\%$). The stress in the Mo on SiO_2 film deposited at 250 W is tensile, whereas the stress in the same Mo film deposited on a Si substrate is compressive. The Pt film shows a high compressive stress. The stress in the top electrode and active AlN as seen in Figure 5(b) shows a strong material dependence. Figure 5(d) depicts the resistivity of the bottom electrode layer as a function of its thickness. Both thickness and resistivity show a large standard deviation in all cases. It is important to note that the two are linearly correlated, since the resistivity has been determined by multiplying the sheet resistance by the film thickness. The Mo film deposited at 1000 W shows a higher thickness and resistivity than other Mo films. The Mo film resistivity is four to six times higher than the bulk resistivity found in literature [6], which is 5.34 $\mu\Omega \cdot cm$ at room temperature. Martin et al. [8] found a Mo film resistivity, which is comparable to the resistivity found in this work.

In Figure 6(a) the relative mean sputtering power for the bottom electrode as compared to the desired sputtering power is plotted against the value of the sputtering power fed to the machine. The relative sputtering power can be seen to linearly decrease with increasing power. For a desired sputtering power of 1000 W the actual mean sputtering power during the deposition was only 72% of the 1000 W. Figure 6(b) shows the measured thickness relative to the desired thickness compared to the relative deposition power. The Mo film deposited at 1000 W had the lowest relative sputtering power but nevertheless the largest thickness.

Figure 7(a) shows the stress found in the 15 nm AlN seed layer on different substrates. The compressive stress can be seen to be largest on SiO_2 with a value of 3.44 GPa and smallest on

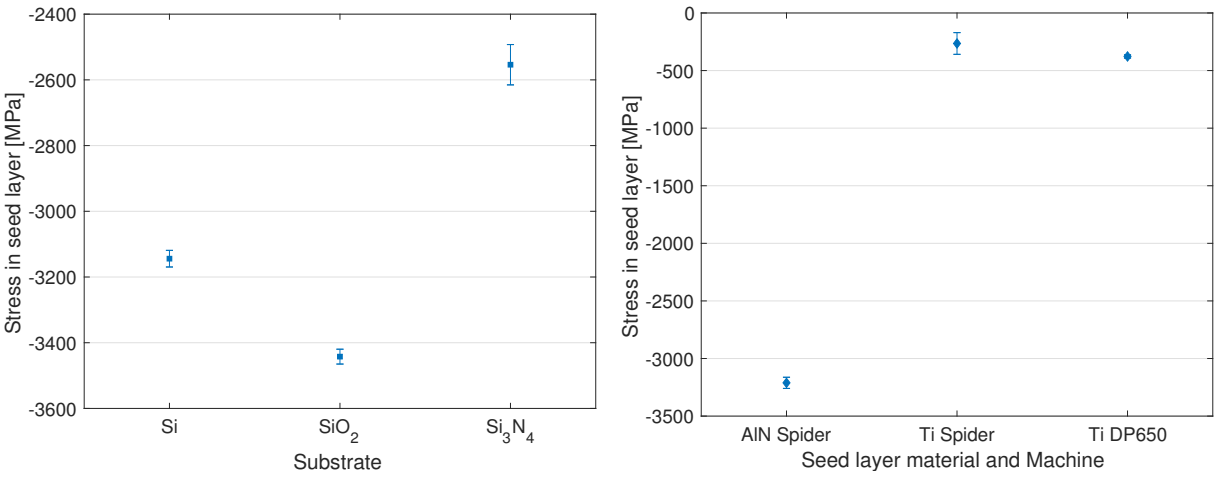

Figure 7: *(a) The stress in the seed layer for different materials and deposition machines. (b) The stress in the AlN adhesion layer on different substrates*

Si_3N_4 with a value of 2.55 GPa. The thickness of these layers is shown in Table 5.

Figure 7(b) shows the stress for different seed layers deposited in different machines. The stress in the AlN seed layer deposited in the Spider is comparable to the value found in Figure 7(a) at 3.21 GPa compressive stress. The stress in the Ti seed layers on the other hand is far lower. It is slightly larger for the one deposited in the DP650 (370 MPa compressive) as in the Ti layer deposited in the Spider (260 MPa compressive). The thickness of these films is indicated in Table 5 as well. It is worth noting the large value of the standard deviation of the seed layer thickness found for wafer 68732. The seed layer thickness of wafers 68732 and 68737 were measured with the DektakXT profilometer, whereas the thickness of the AlN seed layers was measured using the Sopra ellipsometer.

Wafer	**Substrate**	**Seed layer**	**Machine**	**Seed layer thickness [nm]**
73954	Si	AlN	Spider	19.9 ± 0.2
66210	SiO_2	AlN	Spider	18.0 ± 0.1
63228	Si_3N_4	AlN	Spider	15.2 ± 0.5
52442	SiO_2	AlN	Spider	21.5 ± 0.5
68732	SiO_2	Ti	Spider	13 ± 5
68737	SiO_2	Ti	DP650	19.2 ± 0.9

Table 5: *Seed layer thickness for different materials, substrates and machines*

3.3 Variation of seed layers and sputtering machines

Figure 8(a) shows the AlN rocking curve FWHM and the bottom electrode rocking curve FWHM. Figure 8(b) shows the thickness and resistivity of the bottom electrode and Figure 9 shows the stress in (a) the bottom electrode layer and (b) the top electrode and active AlN layers. From these figures can be read that wafers with a Pt bottom electrode show the smallest AlN rocking curve FWHM and the largest compressive stress in the bottom electrode. The stress in the top

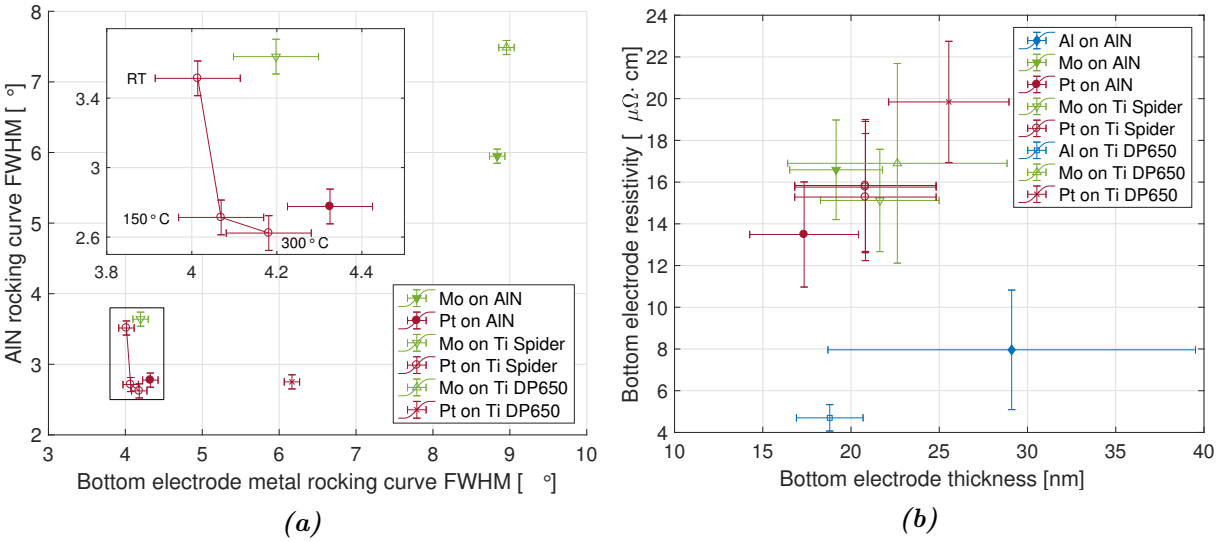

(a) *(b)*

Figure 8: *(a) The rocking curve FWHM from the AlN against the rocking curve FWHM from the bottom electrode metal. The temperatures noted correspond to the active AlN deposition temperatures. The wafers where no temperature is noted have the active AlN layer deposited at 300° C.(b) The bottom electrode resistivity plotted against its thickness.*

electrode and the active AlN is in between the values found for wafers with a Mo and Al bottom electrode. The Mo bottom electrode wafers show a large difference for the AlN rocking curve FWHM. The Mo on Ti deposited in the Spider produced an AlN rocking curve FWHM below 4°. Whereas AlN FWHM of the Mo on Ti deposited in the DP650 and the Mo on AlN were both 6° or higher. The results for the Mo on AlN wafer are comparable to what was found in the second deposition (see Section 3.2), with exception of the stress in the bottom electrode, which is more than ten times larger. The Al bottom electrode produced a very weak peak in the XRD and no rocking curve measurement could be performed. The resistivity is comparable to what was found in the second deposition. The bottom electrode thickness is lower than the 25 *nm* predicted for most samples. The standard deviations of the thickness measurements are rather large with a maximum of 35% for the Al on AlN wafer. The Mo on Ti sample produced in the DP650 resulted in the worst AlN rocking curve. Pt on Ti samples all showed a comparable AlN rocking curve, no matter the seed layer or the deposition machine. The wafer with the Al bottom electrode deposited in the DP650 produced a smaller AlN rocking curve FWHM than the wafer with the Al bottom electrode deposited in the Spider.

3.4 Active AlN deposition temperature variation

Looking at the Pt on Ti wafers deposited in the Spider in Figure 8(a) and Figure 9(b), it can be seen that the AlN rocking curve FWHM does not change significantly between 300°C and 150°C. The AlN rocking curve FWHM of the wafer with the active AlN deposited at room temperature is about 1° larger. The bottom electrode rocking curve does not significantly change for a variation of the active AlN deposition temperature. The stress in the active AlN and top electrode layer can be seen to become more compressive for a lower active AlN deposition temperature.

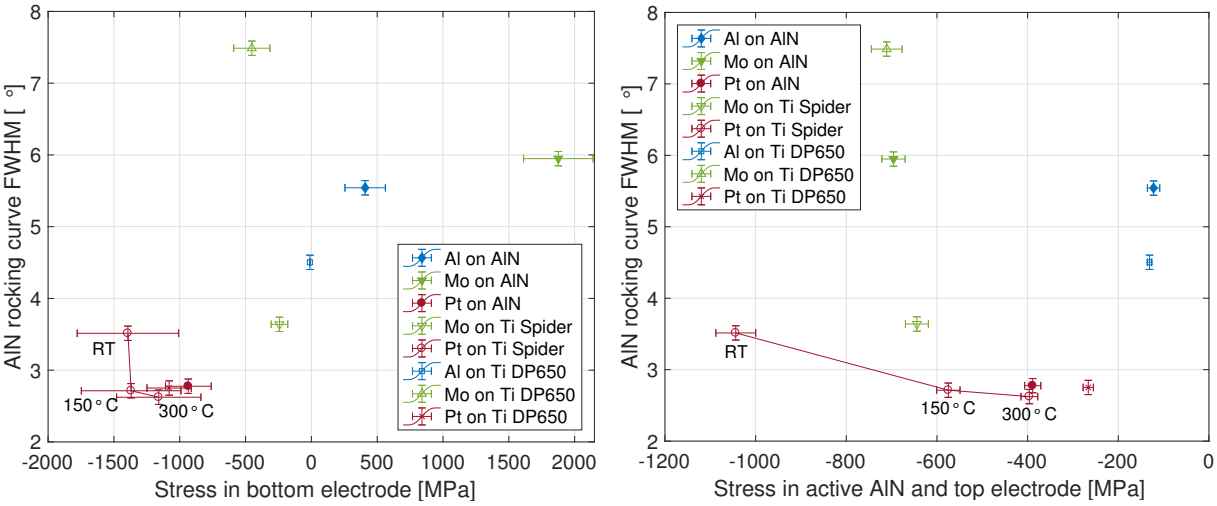

(a) *(b)*

Figure 9: *The rocking curve FWHM of AlN (a) against the stress in the bottom electrode metal layer and (b) against the stress in the AlN and top electrode layer of samples with different bottom electrodes and the bottom electrodes being deposited in two different machines. The indicated numbers correspond to the deposition temperature of the active AlN. Where no temperature is indicated, the active AlN has been deposited at 300° C.*

3.5 Lift-off and thickness measurements

Figure 10(a) shows the end of the wafer 66209 (Al bottom electrode on AlN seed layer) where it was held with the tweezers. The scratch marks from the tweezers are clearly visible with the unaided eye. Figure 10(b) shows the area on the same wafer, where the lift-off was performed. The Al surrounding the lift-off area got heavily scratched by the scrubbing with the cleanroom swab. The scratches are also visible in the profilometer measurement as can be seen in Figure 11(b). As a consequence the standard deviation of the thickness measurement for this wafer is rather large (24%). To reduce these problems in further measurements, wafer 74089 (Al bottom electrode on AlN seed layer) was left in the ultrasonic bath for one hour. Since this only partially removed the Al layer, the wafer was subsequently scrubbed as little as possible. Figure 10(c) shows a microscope image of this wafer. On the left side of this image minor scratches on the Al layer can be seen due to the scrubbing. On the right side the scrub direction of the cleanroom swab can be seen on the Al residues, which are still present. Large Al residues that are still attached to the Al film are also visible. These problems only occurred on Al bottom electrodes.

Another problem with the thickness measurements on the profilometer, was its inaccuracy at steps in the range of tens of nanometer. Looking at Figure 11(c) and (d), a bend can be seen in the profile. This bend was seen over a large number of measurements. Not only is there a bend in the profile, but there is also a trend that measurements running down over the step are in general larger, than measurements running up over the step, as seen in this case, where the measurement running down (Figure 11(c)) yields a step height ($h = 21.61\,nm$) than the measurement running up (Figure 11(d), $h = 9.137\,nm$). The bend could possibly be reduced by tuning the stylus force in the profilometer, which was not done during this project. Another approach to improve measurement accuracy could be to use atomic force microscopy for the step measurements, which is more accurate.

(a)

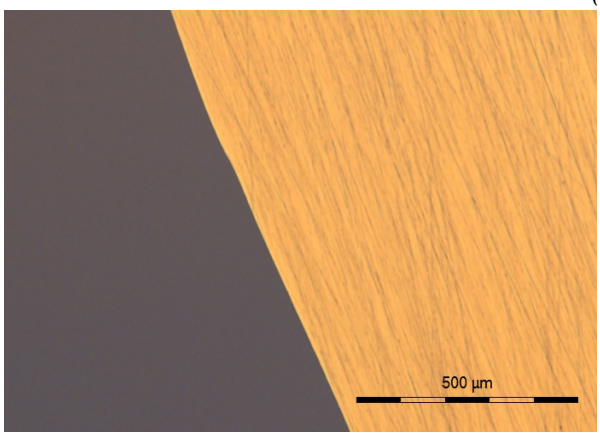

(b)

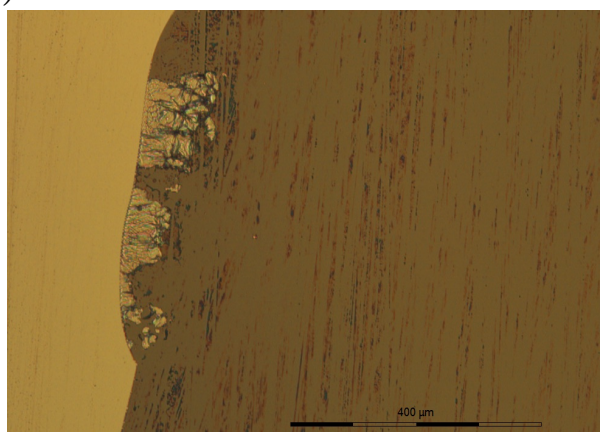

(c)

Figure 10: *(a) is a photo of the end of a wafer with an Al bottom electrode (66209) before depositing the active AlN. (b) is a microscope image of an area on the same wafer, where a lift-off has been performed taken with a 5x magnification, (c) shows again an area where a lift-off has been performed on a different wafer with an Al bottom electrode (74089) taken with a 10x magnification.*

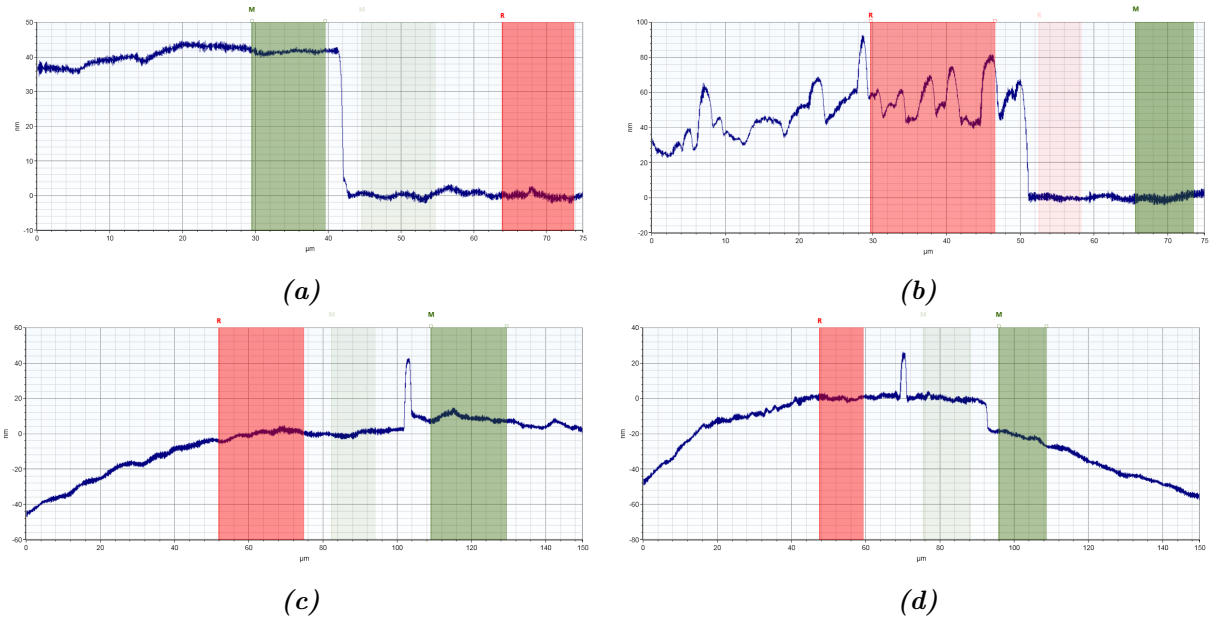

(a) *(b)* *(c)* *(d)*

Figure 11: *A (a) good and a (b) bad example of thickness measurements with the DektakXT. (a) wafer 73955 and (b) wafer 66209. (c) and (d): Dektak profilometer scans from a wafer with only a Ti seed layer deposited in the Pfeiffer-Vacuum spider (Wafer number 68732). (c) yielded a step height of 21.61 nm and (d) a step height of 9.137 nm.*

4 Discussion

4.1 Bottom electrode

The results showed an influence of the underlying layers on the active AlN quality. The Pt on Ti deposited in the Spider on a SiO_2 substrate produced the best result in terms of AlN and bottom electrode rocking curve FWHM (2.6° and 4.2° for AlN and Pt respectively). The Al peaks in the $\theta/2\theta$ scans were not good enough to permit a rocking curve measurement, which indicates a bad crystalline quality. Dubois et al. [2] observed, that the piezoelectric and crystalline quality of the AlN depends on the crystalline quality of the underlying layer, which explains the bad AlN rocking curve FWHM for the Al wafers. The high AlN rocking curve FWHM found on the wafers with the Mo bottom electrodes can be explained by the lack of hexagonal symmetry in the Mo films. The sputtering power used in the deposition of the Mo bottom electrode film does not seem to significantly influence the piezoelectric quality of the AlN film. What it does influence is the in-plane stress in the metal layer. The second wafer with the Mo bottom electrode deposited on the AlN adhesion layer shows a very high tensile stress in the metal layer that does not agree with the results from wafer 66208 previously deposited under the same conditions and this measurement should be repeated to have more reliable data.

4.2 Substrates

The sample on the Si_3N_4 substrate showed by far the worst AlN rocking curve FWHM at 13.0°. Martin et al. [9] showed that a larger AlN film thickness should lead to a better AlN rocking curve FWHM. Given that the active AlN layer on this wafer was three times as thick as on all

the other wafers, would then mean that the AlN rocking curve would be even worse for an AlN layer of 100 nm like on the other wafers. Jakkaraju et al. [4] identified the smoothness of the substrate as an important factor for producing AlN films with a good crystalline quality. Thus the far rougher surface of the Si_3N_4 on polysilicon explains the bad rocking curve results of this wafer. The Mo on Si layer showed a worse rocking curve both for AlN and the bottom electrode. The bottom electrode rocking curve FWHM was around 30% wider than for the Mo on SiO_2. This indicates that SiO_2 is better suited as a substrate for depositing piezoelectric AlN films.

4.3 Adhesion layers

For both Mo and Pt as bottom electrode metals, a better metal rocking curve FWHM was obtained for the samples deposited in the Spider. The Pt samples only showed a slightly worse AlN rocking curve FWHM from the DP650 (2.8°) compared with the Spider (2.6°). The AlN rocking curve obtained for the Mo sample deposited in the DP650 (7.5°) on the other hand is more than twice as large as the one obtained for the sample deposited in the Spider (3.6°). Comparing wafers with an AlN seed layer to wafers with a Ti adhesion layer, it can be seen that the Ti produces more favorable results. The stress in the bottom electrode layer is more compressive in films deposited on Ti seed layers.

4.4 Active AlN deposition temperature

The most interesting result from this work is the change of crystalline quality with changing deposition temperature of the active AlN film. The rocking curve FWHM of the AlN film deposited at 150°C shows no significant difference to the one from the film deposited at 300°C with the underlying layers being identical. The wafer with the same underlying layers and the active AlN deposited at room temperature presents clearly a higher rocking curve FWHM. If it is possible to obtain the same quality in the AlN without heating the deposition chamber and the substrate to 300°C, the time used for the deposition of this film could be considerably reduced. This would also reduce the cost, and another advantage could be the integration of this process with other processes that require lower temperatures.

4.5 Sputter deposition power

For higher sputter deposition powers the deposition time is shorter. The machine will not take less time to reach a higher deposition power. And since the Spider sputtering machine does not have a mechanical shutter over the sample before starting the deposition, the time during which it deposits material (i.e. the deposition time set by the operator) will start running before the desired sputtering power is reached. This might not be of big importance if the deposition time is long, but since for this project the deposition times have been as short as 7 seconds, this might lead to the average deposition power being smaller than what is desired. Since the target power is not stabilized prior to starting the deposition, depositions with higher power and shorter deposition times will be less repeatable and have a larger error in the actual thickness. The DP650 has a mechanical shutter and can therefore control the deposition power more precisely before starting the deposition.

4.6 Aluminum bottom electrode

Al has a number of advantages over other materials tested during this project, mainly its cost and high electrical conductivity. On the other hand it also has drawbacks such as its bad chemical and mechanical resistance. The lift-off did not work very well and hence the thickness measurements are inaccurate. The peak obtained from the $\theta/2\theta$ measurements is too faint to determine the rocking curve. This has to be considered when using Al as a bottom electrode. It might be a good idea to try a different lift-off method for future work.

5 Conclusion

Depositing active AlN films on different bottom electrodes, the influence of many parameters on the active AlN quality was found. The best AlN rocking curve FWHM was measured in a wafer with a Pt bottom electrode and a Ti seed layer deposited in the Spider 600. With this procedure a 2.6° AlN rocking curve FWHM and a 4.2° Pt rocking curve FWHM have been achieved.

- The influence of the bottom electrode material and quality on the AlN crystalline quality could be confirmed. The AlN with the lowest rocking curve FWHM can be grown on a smooth layer with a hexagonal geometry. AlN films grown on (111) Pt produced better results than films grown on (110) Mo and (111) Al. Si_3N_4 on polysilicon was found to be not suitable as a substrate, due to its roughness.
- An effect of the seed layer could be seen on the active AlN quality, where Ti resulted in smaller rocking curve FWHM than AlN.
- The deposition power of the bottom electrode in the case of Mo seemed to have a low influence on the active AlN quality, but will change the stress in the Mo film. A lower deposition power will produce a more precise and repeatable film thickness.
- It was found that the AlN rocking curve FWHM does not change significantly if the active AlN layer is deposited at 300°C or at 150°C.
- Al was found to be difficult to manipulate due to its bad chemical and mechanical stability. No AlN films of satisfactory quality could be grown on Al bottom electrodes.
- A linear dependence of the deposition rate on the sputtering power of Mo films was found.

In a next step more in depth experiments should be made, to find out how the active AlN quality changes for various deposition temperatures of the active AlN film. And since in the scope of this project the only indicator for the piezoelectric quality was the AlN rocking curve, piezoelectric structures should be implemented in order to find the actual piezoelectric response.

6 Appendix

Abbreviations used in the following section: SL: Seed layer, BE: Bottom electrode, AAlN: Active AlN, TE: Top electrode

A First deposition

Wafer number	Machine	Desired sputtering power [W]	Actual sputtering power [W]	Ar gas flow rate [sccm]	Pressure [mbar]	Deposition time [s]	Film thickness [nm]	Stress [MPa]
66726	Spider	250	246.1807629	4.999492537	1.97E-03	60	51 ± 5	75 ± 6
66725	Spider	500	485.9917081	5.002776451	1.97E-03	60	110 ± 3	-260 ± 5
67454	Spider	750	725.092869	4.99831675	1.97E-03	60	162 ± 9	-410 ± 20
66727	Spider	1000	969.8177258	4.999865662	1.97E-03	60	213 ± 2	-523 ± 5

Table A1: *Deposition conditions for the Mo film*

B Second deposition

Wafer number	Substrate	Seed layer	Bottom electrode metal	Top electrode metal	Desired SL thickness [nm]	Desired BE thickness [nm]	Desired AAlN thickness [nm]	Desired TE thickness [nm]	Desired sputtering power BE [W]
66208	SiO_2	AlN	Mo	Al	15	25	100	100	250
66207	SiO_2	AlN	Mo	Al	15	25	100	100	500
66216	SiO_2	AlN	Mo	Al	15	25	100	100	750
66218	SiO_2	AlN	Mo	Al	15	25	100	100	1000
66209	SiO_2	AlN	Al	Mo	15	25	100	100	200
73955	Si	AlN	Mo	Al	15	25	100	100	250
63229	Si_3N_4	AlN	Pt	Mo	15	50	300	50	500
66210	SiO_2	AlN	-	-	15	-	-	-	-
73954	Si	AlN	-	-	15	-	-	-	-
63228	Si_3N_4	AlN	-	-	15	-	-	-	-

Table B1: *A summary of the deposited layers and the desired specifications.*

Wafer number	Desired sputtering power [W]	Actual sputtering power [W]	Ar gas flow rate [sccm]	Pressure [mbar]	Deposition time [s]
66208	250	241.744	4.9998	1.98E-03	29
66207	500	434.532	4.99	2.00E-03	14
66216	750	576.871	5.0046	2.00E-03	9
66218	1000	721.417	5.0025	2.00E-03	7
66209	200	202.181	15.0022	6.36E-03	44
73955	250	241.747	5.0009	1.98E-03	29
63229	500	452.816	5.0033	1.97E-03	22

Table B2: *Deposition conditions for the bottom electrode*

Wafer number	N_2 gas gas flow [sccm]	Ar gas gas flow [sccm]	Pressure [mbar]	DC bias [V]	Forward power [W]	Reflected power [W]	Deposition time [s]	Deposition temperature [°C]
66208	39.9993	10.0002	5.49E-03	86.4985	5.0586	1.65E-04	105	303.4362512
66207	40.0002	9.9999	5.49E-03	82.636	4.9814	0	105	303.5739296
66216	40.0003	9.999	5.48E-03	83.0733	5.1847	0	105	303.5739296
66218	39.9987	9.9993	5.48E-03	82.7108	5.2916	0	105	303.3216936
66209	40.0013	10.0002	5.54E-03	84.2978	4.9221	0	105	303.3467174
73955	40.0005	9.9997	5.49E-03	81.22	4.9958	0	105	303.6036156
63229	40.0008	9.9998	5.40E-03	82.4052	5.1005	0	360	301.2640456

Table B3: *Deposition conditions for the active AlN film*

Wafer number	SL thickness [nm]	BE thickness [nm]	AAlN & TE thickness [nm]	SL stress [MPa]	BE stress [MPa]	AAlN & TE stress [MPa]	SL & BE stress [MPa]	Resistivity [$\mu\Omega \cdot cm$]	Sheet resistance [Ω/sq]
66208	18.0 ± 0.1	22 ± 5	$100 + 100 \pm 5$	-3440 ± 20	150 ± 40	-1500 ± 100	-720 ± 40	190 ± 50	8.6 ± 0.4
66207	18.0 ± 0.1	19 ± 5	$100 + 100 \pm 5$	-3440 ± 20	-40 ± 10	-170 ± 180	-680 ± 40	180 ± 50	9.5 ± 0.4
66216	18.0 ± 0.1	22 ± 4	$100 + 100 \pm 5$	-3440 ± 20	-490 ± 90	-18 ± 100	-700 ± 30	230 ± 40	10.4 ± 0.5
66218	18.0 ± 0.1	30 ± 2	$100 + 100 \pm 5$	-3440 ± 20	-430 ± 30	-1550 ± 50	-670 ± 20	310 ± 30	10.3 ± 0.4
66209	18.0 ± 0.1	25 ± 6	$100 + 100 \pm 5$	-3440 ± 20	310 ± 80	-1300 ± 100	-77 ± 6	70 ± 20	2.9 ± 0.1
73955	19.9 ± 0.2	21 ± 2	$100 + 100 \pm 5$	-3140 ± 30	-44 ± 4	-1550 ± 40	-740 ± 30	200 ± 20	9.7 ± 0.8
63229	15.2 ± 0.5	50 ± 5	$300 + 50 \pm 5$	-2550 ± 60	-890 ± 50	-1280 ± 40	-130 ± 3	190 ± 10	3.8 ± 0.2
66210	18.0 ± 0.1	-	-	-	-3440 ± 20	-	-3440 ± 20	-	-
73954	19.9 ± 0.2	-	-	-	-3140 ± 30	-	-3140 ± 30	-	-
63228	15.2 ± 0.5	-	-	-	-2550 ± 60	-	-2550 ± 60	-	-

Table B4: *A summary of the measurement and calculation results excluding the XRD results presented in a different table*

Wafer number	AlN θ position [°]	AlN θ FWHM [°]	AlN rocking curve FWHM [°]	BE metal θ position [°]	BE metal FWHM [°]	BE metal rocking curve FWHM[°]
66208	36.0	0.315	6.2 ± 0.1	40.	0.548	9.0 ± 0.1
66207	36.02	0.31	6.0 ± 0.1	40.44	0.583	8.7 ± 0.1
66216	36.01	0.326	6.3 ± 0.1	40.41	0.625	9.4 ± 0.1
66218	36.01	0.302	6.3 ± 0.1	40.4	0.612	9.3 ± 0.1
66209	36.02	0.39	8.0 ± 0.1	40.69	0.303	-
73955	36	0.324	7.1 ± 0.1	40.47	0.593	11.6 ± 0.1
63229	36.05	0.256	13.0 ± 0.1	39.89	0.391	16.3 ± 0.1

Table B5: *Summary of XRD measurements*

C Third deposition

Wafer number	Substrate	Machine	Seed layer	Bottom electrode metal	Top electrode metal	Desired SL thickness [nm]	Desired BE thickness [nm]	Desired AAlN thickness [nm]	Desired TE thickness [nm]	Desired sputtering power BE [W]
74089	SiO_2	Spider	AlN	Al	Mo	15	25	100	100	200
74086	SiO_2	Spider	AlN	Mo	Al	15	25	100	100	250
74088	SiO_2	Spider	AlN	Pt	Al	15	25	100	100	500
68734	SiO_2	Spider	Ti	Mo	Al	15	25	100	100	250
68733	SiO_2	Spider	Ti	Pt	Al	15	25	100	100	500
68738	SiO_2	Spider	Ti	Pt	Al	15	25	100	100	500
68739	SiO_2	Spider	Ti	Pt	Al	15	25	100	100	500
68736	SiO_2	DP650	Ti	Al	Mo	15	25	100	100	400
68735	SiO_2	DP650	Ti	Mo	Al	15	25	100	100	400
74087	SiO_2	DP650	Ti	Pt	Al	15	25	100	100	250
52442	SiO_2	Spider	AlN	-	-	15	-	-	-	-
68732	SiO_2	Spider	Ti	-	-	15	-	-	-	-
68737	SiO_2	DP650	Ti	-	-	15	-	-	-	-

Table C1: *A summary of the deposited layers and the desired specifications.*

Wafer number	Desired sputtering power [W]	Actual sputtering power [W]	Ar gas flow rate [sccm]	Pressure [mbar]	Deposition time [s]
74089	200	198.0519187	14.99854966	6.36E-03	44
74086	250	240.6601942	4.999420065	1.99E-03	31
74088	500	412.6880734	5.003756881	1.97E-03	11
68734	250	240.8673139	5.001957282	1.97E-03	31
68733	500	410.1203704	5.008476852	1.98E-03	11
68738	500	415.4954128	5.002778704	1.97E-03	11
68739	500	414.2110092	5.000323148	1.99E-03	11
68736	400	-	-	-	-
68735	400	-	-	-	-
74087	250	-	-	-	-

Table C2: *Deposition conditions for the bottom electrode*

Wafer number	N_2 gas gas flow [sccm]	Ar gas gas flow [sccm]	Pressure [mbar]	DC bias [V]	Forward power [W]	Reflected power [W]	Deposition time [s]	Deposition temperature [°C]
74089	39.99816067	10.00005871	5.34E-03	85.9526421	5.092702717	0	105	303.2285442
74086	39.99976775	10.0009902	5.36E-03	84.43672472	5.010026826	0	105	301.1189343
74088	39.99969153	10.00029467	5.33E-03	86.7441612	5.07775333	0	105	301.3281905
68734	40.00109924	10.00120856	5.34E-03	86.56052877	5.13086082	0	105	300.4727619
68733	40.00100143	10.00003064	5.36E-03	89.97355913	5.085896164	0	105	34.97859182
68738	39.99990305	10.00010667	5.33E-03	88.42779982	5.238975447	0	105	152.7956232
68739	40.00071361	9.99912255	5.37E-03	87.73197704	5.010274606	0	105	301.405138
68736	39.9997099	10.00062067	5.34E-03	84.8913733	4.90942819	0.00024778	105	303.4951475
68735	39.99946371	10.00026232	5.35E-03	85.52332214	5.123675204	0.000165187	105	303.0062797
74087	39.99932483	9.998553853	5.39E-03	84.46331977	5.081470029	8.26E-05	105	301.37098

Table C3: *Deposition conditions for the active AlN film*

Wafer number	SL thickness [nm]	BE thickness [nm]	AAlN & TE thickness [nm]	SL stress [MPa]	BE stress [MPa]	AAlN & TE stress [MPa]	SL & BE stress [MPa]	Resistivity [$\mu\Omega \cdot cm$]	Sheet resistance [Ω/sq]
74089	21.5 ± 0.5	29 ± 10	$100 + 100 \pm 5$	-3210 ± 50	410 ± 150	-120 ± 10	-1100 ± 200	8 ± 3	2.7 ± 0.1
74086	21.5 ± 0.5	19 ± 3	$100 + 100 \pm 5$	-3210 ± 50	1900 ± 260	-700 ± 30	-810 ± 40	17 ± 2	8.7 ± 0.4
74088	21.5 ± 0.5	17 ± 3	$100 + 100 \pm 5$	-3210 ± 50	-900 ± 200	-390 ± 20	-2200 ± 100	13 ± 3	7.8 ± 0.4
68734	14 ± 5	22 ± 3	$100 + 100 \pm 5$	-260 ± 90	-240 ± 60	-640 ± 30	-250 ± 20	15 ± 2	7.0 ± 0.3
68733	14 ± 5	21 ± 4	$100 + 100 \pm 5$	-260 ± 90	-1400 ± 400	-1040 ± 40	-950 ± 80	16 ± 3	7.6 ± 0.4
68738	14 ± 5	21 ± 4	$100 + 100 \pm 5$	-260 ± 90	-1400 ± 400	-570 ± 30	-930 ± 80	15 ± 3	7.3 ± 0.4
68739	14 ± 5	21 ± 4	$100 + 100 \pm 5$	-260 ± 90	-1200 ± 300	-400 ± 20	-800 ± 70	16 ± 3	7.6 ± 0.4
68736	19.2 ± 0.9	19 ± 2	$100 + 100 \pm 5$	-380 ± 10	-11.3 ± 1.2	-131.0 ± 4.7	-196 ± 8	4.7 ± 0.6	2.5 ± 0.2
68735	19.2 ± 0.9	23 ± 6	$100 + 100 \pm 5$	-380 ± 10	-500 ± 100	-710 ± 30	-420 ± 40	17 ± 5	7.5 ± 0.5
74087	19.2 ± 0.9	26 ± 3	$100 + 100 \pm 5$	-380 ± 10	-1100 ± 200	-270 ± 10	-780 ± 40	20 ± 3	7.8 ± 0.5
52442	21.5 ± 0.5	-	-	-3210 ± 50	-	-	-3210 ± 50	-	-
68732	14 ± 5	-	-	-260 ± 90	-	-	-260 ± 90	150 ± 60	108 ± 4
68737	19.2 ± 0.9	-	-	-380 ± 10	-	-	-380 ± 10	140 ± 10	70 ± 5

Table C4: *A summary of the measurement and calculation results excluding the XRD results presented in a different table*

Wafer number	AlN θ position [°]	AlN θ FWHM [°]	AlN rocking curve FWHM [°]	BE metal θ position [°]	BE metal FWHM [°]	BE metal rocking curve FWHM[°]
74089	35.93	0.364	5.5 ± 0.1	40.59	0.436	-
74086	35.85	0.314	5.9 ± 0.1	40.34	0.575	8.8 ± 0.1
74088	-	0.216	2.8 ± 0.1	-	0.489	4.3 ± 0.1
68734	35.97	0.251	3.6 ± 0.1	40.53	0.443	4.2 ± 0.1
68733	35.83	0.255	3.5 ± 0.1	39.62	0.523	4.0 ± 0.1
68738	-	0.217	2.7 ± 0.1	-	0.532	4.1 ± 0.1
68739	-	0.22	2.6 ± 0.1	-	0.483	4.2 ± 0.1
68736	-	0.322	4.5 ± 0.1	-	1.739	-
68735	35.96	0.332	7.5 ± 0.1	40.42	0.524	9.0 ± 0.1
74087	35.86	0.23	2.8 ± 0.1	39.85	0.554	6.2 ± 0.1

Table C5: *Summary of XRD measurements*

D Standard deviation calculations

The following section gives an overview of the calculation of the standard deviation, when error propagation was required.

D.1 Stress

Stress was calculated with Stoney's formula

$$\sigma = \frac{E_{subst}}{6(1-\nu_s)}\frac{t_s^2}{t_f}\cdot\left[\frac{1}{R}-\frac{1}{R_0}\right] \tag{5}$$

where the film thickness t_f, radius of curvature R and radius of curvature before deposition R_0 were measurement results. s_t, s_R and s_{R0} are the corresponding standard deviations. All other parameters were supposed exactly known. From this the standard deviation of the stress s_σ can be found

$$s_\sigma = \sigma\cdot\sqrt{\left(\frac{s_t}{t_f}\right)^2+\left(\left(\frac{s_R}{R^2}\right)^2+\left(\frac{s_{R0}}{R_0^2}\right)^2\right)/\left[\frac{1}{R}-\frac{1}{R_0}\right]} \tag{6}$$

If the stress in two layers combined and in one of them is known, the stress in the other layer is found by

$$\sigma_2 = \frac{\sigma_{12}t_{12}-\sigma_1 t_1}{t_2} \tag{7}$$

with t designating the thickness and σ the film stress. Then the standard deviation can be found

$$s_{\sigma 2} = \sigma_2\cdot\sqrt{\left(\frac{s_{t2}}{t_2}\right)^2+\frac{\left(\left(\frac{s_{\sigma 12}}{\sigma_{12}}\right)^2+\left(\frac{s_{t12}}{t_{12}}\right)^2\right)\cdot\sigma_{12}^2t_{12}^2+\left(\left(\frac{s_{\sigma 1}}{\sigma_1}\right)^2+\left(\frac{s_{t1}}{t_1}\right)^2\right)\cdot\sigma_1^2t_1^2}{\left(\sigma_{12}t_{12}+\sigma_1t_1\right)^2}} \tag{8}$$

D.2 Resistivity

The resistivity was found from the sheet resistance R_s as

$$\rho = R_s\cdot t_f \tag{9}$$

The standard deviation can then be found

$$s_\rho = \rho\cdot\sqrt{\left(\frac{s_{Rs}}{R_s}\right)^2+\left(\frac{s_{tf}}{t_f}\right)^2} \tag{10}$$

References

[1] M. R. Ardigo, M. Ahmed, and A. Besnard. Stoney formula: Investigation of curvature measurements by optical profilometer. In *Residual Stresses IX*, volume 996 of *Advanced Materials Research*, pages 361–366. Trans Tech Publications, 10 2014.

[2] M.-A. Dubois and P. Muralt. Stress and piezoelectric properties of aluminum nitride thin films deposited onto metal electrodes by pulsed direct current reactive sputtering. *Journal of Applied Physics*, 89(11):6389–6395, 2001.

[3] I. Ivanov, L. Hultman, K. Järrendahl, P. Mårtensson, J.-E. Sundgren, B. Hjörvarsson, and J. E. Greene. Growth of epitaxial AlN(0001) on Si(111) by reactive magnetron sputter deposition. *Journal of Applied Physics*, 78(9):5721–5726, 1995.

[4] R. Jakkaraju, G. Henn, C. Shearer, M. Harris, N. Rimmer, and P. Rich. Integrated approach to electrode and AlN depositions for bulk acoustic wave (BAW) devices. *Microelectronic Engineering*, 70(2):566 – 570, 2003. Materials for Advanced Metallization 2003.

[5] H. Jin, B. Feng, S. Dong, C. Zhou, J. Zhou, Y. Yang, T. Ren, J. Luo, and D. Wang. Influence of substrate temperature on structural properties and deposition rate of AlN thin film deposited by reactive magnetron sputtering. *Journal of Electronic Materials*, 41(7):1948–1954, Jul 2012.

[6] D. R. Lide. *CRC Handbook of Chemistry and Physics*. CRC Press, 2005.

[7] H.P. Loebl, M. Klee, C. Metzmacher, W. Brand, R. Milsom, and P. Lok. Piezoelectric thin AlN films for bulk acoustic wave (BAW) resonators. *Materials Chemistry and Physics*, 79(2):143 – 146, 2003. APMC-SSMM Asia-pacific Microwave conference: Special session on microwave materials.

[8] F. Martin, P. Muralt, and M.-A. Dubois. Process optimization for the sputter deposition of molybdenum thin films as electrode for AlN thin films. *Journal of Vacuum Science & Technology A: Vacuum, Surfaces, and Films*, 24(4):946–952, 2006.

[9] F. Martin, P. Muralt, M.-A. Dubois, and A. Pezous. Thickness dependence of the properties of highly c-axis textured AlN thin films. *Journal of Vacuum Science & Technology A: Vacuum, Surfaces, and Films*, 22(2):361–365, 2004.

[10] P. Muralt. AlN thin film processing and basic properties. In H. Bhugra and G. Piazza, editors, *Piezoelectric MEMS Resonators*, pages 1–37. Springer International Publishing Switzerland, 2017.

[11] J. Ph. Piel. Introduction to ellipsometry. online, Oct 2008. `https://cmi.epfl.ch/metrology/files/Sopra\%20GES\%205E/Introduction\%20to\%20ellipsometry.pdf`, accessed Jan 14, 2018.

[12] J. S. Pulskamp, A. Wickenden, R. Polcawich, B. Piekarski, M. Dubey, and G. Smith. Mitigation of residual film stress deformation in multilayer microelectromechanical systems cantilever devices. *Journal of Vacuum Science & Technology B: Microelectronics and Nanometer Structures Processing, Measurement, and Phenomena*, 21(6):2482–2486, 2003.

[13] online. "http://www.pvd.ir/faqs/", accessed Jan 13. 2018.